eprints@whiterose.ac.uk
https://eprints.whiterose.ac.uk/

# Neural Network Adaptive Control of Hand Rehabilitation Robot Driven by Flexible Pneumatic Muscles

Feifei Shao
*School of Information Engineering, Wuhan University of Technology*
Wuhan, China
e-mail: shaofeifei@whut.edu.cn

Wei Meng
*School of Information Engineering, Wuhan University of Technology*
Wuhan, China
email: weimeng@whut.edu.cn

Qingsong Ai
*School of Information Engineering, Wuhan University of Technology*
Wuhan, China
email: qingsongai@whut.edu.cn

Sheng Q. Xie
*School of Electronic and Electrical Engineering, University of Leeds*
Leeds, UK
email: s.q.xie@leeds.ac.uk

*Abstract*—The aim of this study is to design a reliable and stable controller for hand rehabilitation robot driven by flexible pneumatic muscles(FPMs) for post stroke patients. Position control is key to perform effective rehabilitation robotic exercise. However, it is difficult to achieve precise control due to the nonlinearity and hysteresis of the flexible muscles. The efficient control system is required to realize the high-precision control of the joint angle. In this paper, to achieve the stability and anti-interference ability of the system, an improved neural network adaptive control(INNAC) method is proposed. The neural network is used to estimate the unknown items and the adaptive control is used to realize the adaptive characteristics in the unknown environment, so as to realize the stability and high precision control of the control system when encountering human interferences. Finally, experiments were carried out on robot with human participants for five fingers movement assistance. The results show that the control system can achieve good control effect and anti-interference ability.

*Keywords—neural network, flexible pneumatic muscles, robotics, adaptive control*

## I. INTRODUCTION

With the improvement of people's living standards, the incidence of paralysis and stroke also increases. According to the World Health Organization (WHO) report that about 39.4% population of the world become aged by 2060 which may cause their muscle deterioration and difficulties in walking and performing activities of daily lives [1], while stroke, as a high incidence of aging population, will continue to rise in the number of stroke patients in the future. Besides that, it is also reported by WHO that among the top 10 causes of death in the world in 2016, stroke ranks the second [2]. Therefore, the rehabilitation of patients after stroke has become a problem worthy of attention. In the traditional rehabilitation treatment, the therapist performs one-to-one rehabilitation treatment on patients. This method is not only labor-intensive and expensive, but also difficult to guarantee the training efficiency and intensity [3]. The applications of rehabilitation robotics are not limited and can help stroke patients recover from injury more quickly [4].

Rigid rehabilitation robots are not conducive to long-term rehabilitation training for patients due to their poor comfort, poor portability and the possibility of causing secondary injuries to patients [5]. Compared with rigid actuator, flexible pneumatic muscles(FPMs) are more compliant and safer. The use of them as actuators meets the requirements of safety, portable, flexible and comfort during the rehabilitation process [6]. In addition, The FPMs are simple in structure and convenient to control, which can better help stroke patients with rehabilitation training.

However, due to the nonlinearity, hysteresis and jitter of the FPMs, it is difficult to achieve precise control. Many scholars have carried out relevant researches on improving the position control performance of hand rehabilitation robot. Wang et al. [7,8] used the finite element analysis method to analyze the influencing factors of the fiber-enhanced PMs bending angle, such as length and thickness, and used PID for angle tracking control. Farag et al. [9] modeled the robot finger and FPMs actuator as a nonlinear second-order system based on empirical methods, and designed an adaptive inversion controller that can compensate for the uncertain friction between the actuator and the finger. Chen et al. [10] took PMs as the control object and proposed a T-S fuzzy logic control method based on genetic algorithm optimization. This method can not only realize the basic trajectory tracking control, but also overcome the jitter in the trajectory tracking process and improve the control accuracy. Aiming at the irregularity of the flexible rubber tube actuator and the uncertainty of the disturbance term, Alici et al. [11] designed a nonlinear controller with an uncertain nonlinear model, which effectively reduced the error between the actual output and the estimated output and improved the control effect. Girin et al. [12] applied a high-order sliding mode controller to

practical control. The controller can achieve finite time convergence and eliminate the flutter problem of general sliding mode controllers. Finally, the accurate and fast tracking performance of the controller is proved by experiments. In addition, since different control methods have different advantages and disadvantages, there are examples of combining various control algorithms to control FPMs [13].

Neural network is a neural network computing model based on single neuron model. Its strong learning ability and continuous nonlinear function approximation ability provide an effective way to solve FPMs nonlinear control problems and uncertain model control problems. For example, Wang et al. [14] proposed a neural network controller to achieve robot tracking with a highly nonlinear structure. The simulation results show that it has a better control effect. Robinson et al. [15] combined neural network with adaptive control and proposed an adaptive neural network control method to solve the strong nonlinear problem in the single-joint system driven by PMs. In order to overcome the nonlinear characteristics of pneumatic muscle actuator, Lee et al. [16] designed a sliding mode control algorithm based on neural network, and conducted tracking experiments on the location and speed of the actuator, so as to reduce the jitter of the flexible actuator under the motion state. Therefore, the neural network has a good control effect on robot driven by FPMs.

Considering the nonlinear and uncertain disturbance of the system, an improved neural network adaptive control(INNAC) method is proposed, and the effectiveness of the method is verified by experimental results. The rest of this paper is organized as follows: Section II introduces the design of flexible hand rehabilitation robot based on FPMs and the establishment of dynamic differential equation. Section III designs the control system. In Section IV, the actual control experiment is carried out and the experimental results are analyzed. Then the conclusion is given in Section V.

## II. HAND REHABILITATION ROBOT

### A. Robot Design

The structure of the FPMs are asymmetric corrugated tubular pneumatic drive. The original state and bending state are shown in Fig. 1, under the action of air pressure, due to the difference in rigidity strength between the bottom and the back, the actuator will bend to the side of the back during the inflating stage of the flexible pneumatic muscle. When the actuator deflates, it will gradually return to the original state.
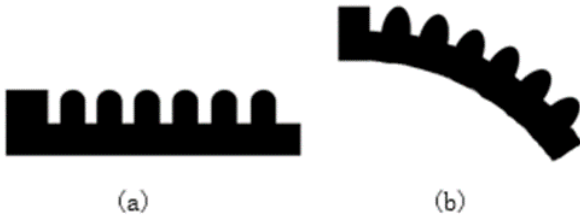


Fig. 1. FPMs: (a) original state (b) bending state.

The flexible hand rehabilitation robot is designed by the FPMs, as shown in Fig. 2. Fig. 2(a) shows the robot designed by FPMs, Fig. 2(b) shows the bending state of the robot worn on

the human hand. The robot uses five FPMs to control the wearer's five fingers, and controls the bending and extension of each finger by controlling the inflation and deflation, so as to assist participants in finger movement training.
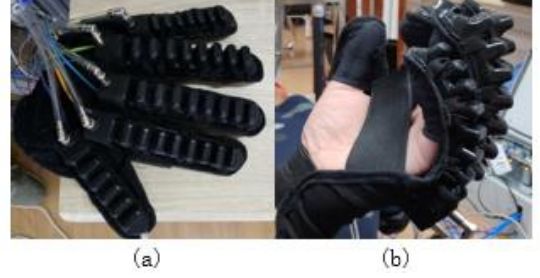


Fig. 2. Flexible hand rehabilitation robot (a) original state (b) bending state.

### B. Dynamic Differential Equation of Actuator

Through the step response experiment, the discrete data points in the time domain that change with time during the step response of the flexible pneumatic muscle driver under different input pressures are obtained. In the step response experiment, the sampling frequency of the angle sensor is 50 Hz, and the sampling time is 3s. A total of 11 sets of step response curves under different air pressures are set. The input signal voltage starts at 1.0v, and the step response is measured once every 0.3v.

Use two real poles to fit the time-domain curve equation of the FPMs actuator step response, and set the system equation as:

$$\theta(t) = A_0 - A_1 e^{-\lambda_1 t} - A_2 e^{-\lambda_2 t} \qquad (1)$$

The fitting results are shown in Table I:

TABLE I. STEP RESPONSE FITTING PARAMETERS

| u | $A_0$ | $A_1$ | $A_2$ | $\lambda_1$ | $\lambda_2$ |
|---|---|---|---|---|---|
| 1.0v | 15.7511 | 3.1652 | 10.3511 | 6.5151 | 0.5457 |
| 1.3v | 21.4130 | 5.0603 | 12.1022 | 7.8712 | 0.5171 |
| 1.6v | 27.9860 | 5.5080 | 12.7930 | 7.2871 | 0.5050 |
| 1.9v | 35.8252 | 4.7610 | 13.3870 | 6.9961 | 0.5212 |
| 2.2v | 39.0741 | 10.0710 | 12.0064 | 7.7185 | 0.5169 |
| 2.5v | 43.8073 | 9.0980 | 15.3540 | 7.0416 | 0.5365 |
| 2.8v | 20.2352 | 5.4921 | 14.0250 | 6.4139 | 0.5257 |
| 3.1v | 48.2262 | 6.0813 | 11.6413 | 7.9498 | 0.4981 |
| 3.4v | 53.1031 | 8.4950 | 14.7232 | 7.0593 | 0.5012 |
| 3.7v | 56.1720 | 6.5161 | 13.5020 | 6.5335 | 0.5254 |
| 4.0v | 61.3410 | 8.1324 | 13.6631 | 5.9687 | 0.5033 |

According to (1), the second-order dynamic differential equation of the FPMs actuator can be expressed as:

$$\ddot{\theta} + (\lambda_1 + \lambda_2)\dot{\theta} + (\lambda_1 \lambda_2)\theta = (\lambda_1 \lambda_2 \theta) \qquad (2)$$

Among them, $A_0$, $A_1$, $A_2$ and $\lambda_1$, $\lambda_2$ are fitted as functions of input voltage u. As follows:

$$A_0 = -2.657u^2 + 27.78u - 9.28 \qquad (3)$$

$$A_1 = -0.9372u^2 + 6.342u - 2.239 \qquad (4)$$

$$A_2 = -0.7212u^2 + 4.45u - 2.239 \qquad (5)$$

$$\lambda_1 = -0.359u + 7.861 \tag{6}$$

$$\lambda_2 = -0.0069u + 0.5349 \tag{7}$$

## III. CONTROL SYSTEM

### A. SNNAC Algorithm

First, a single neuron network adaptive control(SNNAC) algorithm is designed, and its output can be expressed as:

$$u(k) = u(k-1) + K \sum_{i=1}^{3} w_i'(k)x_i(k) \tag{8}$$

$$w_i' = \frac{w_i(k)}{\sum_{i=1}^{3}|w_i(k)|} \tag{9}$$

Here $u(k)$ represents the output signal at time $k$, $w_i(k)$ is the weighted coefficient, $K$ is the proportionality coefficients of neurons, where $K > 0$. The choice of $K$ value is very important. The larger the $K$, the better the speed, but the large overshoot will also make the system unstable. $x_1(k) = e(k)$, $x_2(k) = e(k) - e(k-1)$, and $x_3(k) = e(k) - 2e(k-1) + e(k-2)$. $e(k)$ is the difference value between system input and control output at time $k$.

$$w_1(k) = w_1(k-1) + \eta_I z(k)u(k)x_1(k) \tag{10}$$

$$w_2(k) = w_2(k-1) + \eta_P z(k)u(k)x_2(k) \tag{11}$$

$$w_3(k) = w_3(k-1) + \eta_D z(k)u(k)x_3(k) \tag{12}$$

Where $\eta_I$, $\eta_P$, $\eta_D$, are the learning rates of integration, proportion and differentiation respectively, among them $z(k) = e(k)$.

The above equations together constitute a single neuron adaptive control(SNNAC) system. Assuming that the reference input signal at time $k$ is $\theta_d(k)$, it is substituted into the above control system, and $u(k)$ is used as the control signal of the FPMs to control the bending motion of the robot. The angle sensor is used to collect angle information, the output signal at time $k$ is $\theta(k)$, and the angle error at time $k$ is expressed as $e(k) = \theta_d(k) - \theta(k)$. This method realizes the self-adaptive function by adjusting the weighting coefficients, which is not only simple in structure, but also adaptable to environmental changes and has strong robustness.

### B. INNAC Algorithm

The SNNAC algorithm has higher requirements for neural network parameters and system parameters. If the parameters are not selected properly, the closed-loop control system is easy to diverge. In order to improve the stability of the system, an improved neural network adaptive control(SNNAC) method is introduced here.

First, transform the differential equation of the system into the following form:

$$\ddot{\theta} = f(\theta, \dot{\theta}) + g(\theta, \dot{\theta})u \tag{13}$$

For the above second-order nonlinear system, the ideal control is designed as follows:

$$u = \frac{1}{g(\theta)}\left[-f(\theta) + \ddot{\theta}_d + K^T E\right] \tag{14}$$

Where $\ddot{\theta}_d$ is the second derivative of the ideal trace trajectory, $K = [k_p, k_d]^T$, $E = [e, \dot{e}]^T$, $e$ is the trajectory tracking error.

Use the first-order Taylor formula to approximately simplify higher-order terms to first-order terms:

$$f(u) = f(u_0) + f'(u_0)(u - u_0) \tag{15}$$

Therefore, the differential equation can be transformed into:

$$\ddot{\theta} = f_1(u)\dot{\theta} + f_2(u)\theta + f_3(u)$$

$$= (f_1(u_0)) + f_1'(u_0)(u - u_0)\dot{\theta} +$$

$$(f_2(u_0)) + f_2'(u_0)(u - u_0)\theta +$$

$$(f_3(u_0)) + f_3'(u_0)(u - u_0) \tag{16}$$

Further simplifying (16) can be obtained as follows:

$$\ddot{\theta} = f(\theta, \dot{\theta}) + g(\theta, \dot{\theta})\Delta u, \quad \Delta u = u - u_0 \tag{17}$$

$$f(\theta, \dot{\theta}) = f_1(u_0)\dot{\theta} + f_2(u_0)\theta + f_3(u_0) \tag{18}$$

$$g(\theta, \dot{\theta}) = f_1'(u_0)\dot{\theta} + f_2'(u_0)\theta + f_3'(u_0) \tag{19}$$

In order to realize the stability of the closed-loop system, RBF neural network is used to realize the approximation of function $f(\theta)$. The neural network algorithm is as follows:

$$h_j = exp\left(-\frac{\|x - c_j\|^2}{2b_j^2}\right), \quad j = 1,2,...,m \tag{20}$$

$$f = W^T h(x) + \varepsilon \tag{21}$$

Where $x = [x_1, x_2, ..., x_n]^T$ is the input of the network, and $h_j$ is the output of the j neuron of the hidden layer. $c_j = [c_{j1}, c_{j2}, ..., c_{jn}]$ is the central vector value of the j hidden layer neuron, $h = [h_1, h_2, ..., h_n]^T$ is the output of the Gaussian function, $W$ is the weight of the network, and $\varepsilon$ is the approximation error of the network.

Considering the stability of the system and the possible uncertain interference, INNAC algorithm is designed by combining neural network with adaptive control. Its control law and adaptive law are as follows:

By replacing the output of the neural network with the function $f(\theta)$ in (14), the control output can be obtained as follows:

$$u = \frac{1}{g(\theta)}\left[-\hat{f}(\theta) + \ddot{\theta}_d + K^T E\right] \tag{22}$$

$$\hat{f}(\theta) = \widehat{W}^T h(\theta) \tag{23}$$

Among them, $h(\theta)$ is the Gaussian function, and $\widehat{W}$ is the estimated value of the ideal weight.

The adaptive law is designed as:

$$\widehat{W} = -\gamma E^T PBh(\theta) \qquad (24)$$

Where $P$ and $B$ are setting matrices, and $\gamma$ is an adjustable normal number.
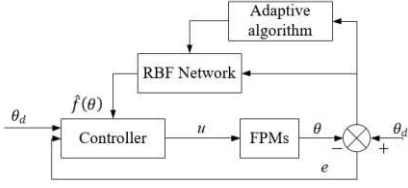


Fig. 3. INNAC system block diagram.

The system block diagram is shown in Fig. 3. This control method takes $u$ as the control voltage signal of the hand rehabilitation robot. The angle signal of the finger is collected in real time through the angle sensor and fed back to the front control system, so as to carry out real-time adaptive adjustment of $u$ and improve the stability and adaptive ability of the system.

## IV. EXPERIMENTS AND RESULTS DISCUSSION

### A. Experimental Setup

Fig. 2 shows the robot designed by the FPMs. Each finger is driven by a FPM, which can assist the hand in collaborative movement, or individually control each finger movement assistance. The INNAC program is written in LabVIEW. Control signal sent by the control program is converted into an analog signal by the data acquisition module (USB-7660BD) and sent to the proportional valve. Finger angles increase and decrease by controlling the inflation and deflation of FPMs. The angle sensor is fixed between the FPMs and the finger. The measured angle signal is converted into digital value through the data acquisition device (NI USB-6210) and sent to the control program.

### B. Experimental Results

Considering the safety of the fingers in the rehabilitation training process, it is necessary to ensure the smooth and slow operation of the control system and the reasonableness of the range of motion. In this experiment, the required control angle signal is set to a sine curve with a frequency of 0.05HZ. Because the thumb and little finger are shorter and the bending angle is smaller, the control signal of the thumb and little finger is set to amplitude smaller sine curve. The angular trajectory of the thumb and little finger is set to 0~70°, and the angular trajectory of the index finger, middle finger and ring finger is set to 0~90°. The angle control result of five fingers is shown in the figure below. The trajectory tracking control effect and error results of the five fingers are given below.

As shown in Fig. 4-8, the angle trajectory and error trajectory of the five fingers are shown respectively. In the angle track curve, the red curve represents the ideal angle track of each finger. The control results of SNNAC and INNAC are represented by blue and green curves respectively. From the experimental results of the angle trajectory of each finger, it can be seen that the INNAC tracking trajectory is closer to the ideal trajectory curve and has a better control effect. In the error curve

diagram, the red curve and the blue curve respectively represent the difference of the angle trajectory controlled by SNNAC and INNAC. It can be seen from the experimental results that the SNNAC control effect is poor, the angle control is unstable, and the error fluctuates greatly at the curve amplitude. The INNAC control effect is better, and the error fluctuation is smaller, and the control effect is more stable.
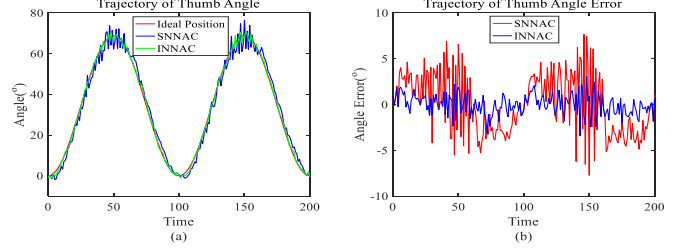


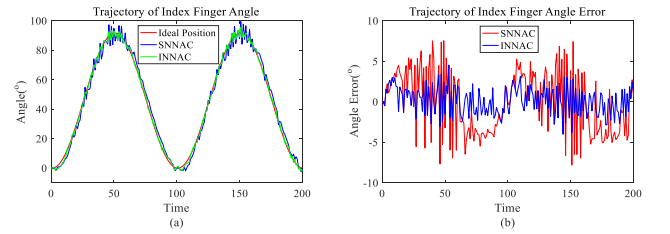Fig. 4. Thumb angle tracking and error result.



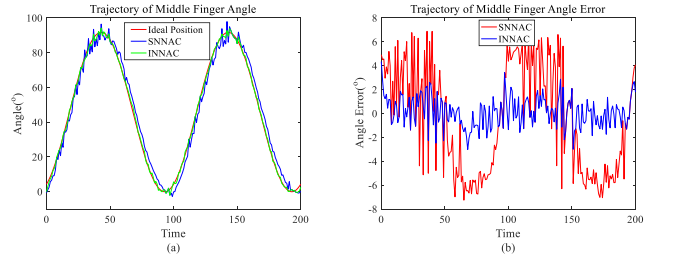Fig. 5. Index finger angle tracking and error result.



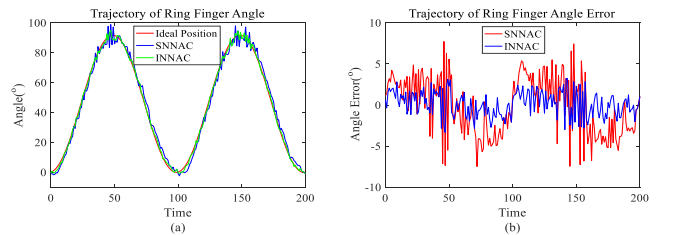Fig. 6. Middle finger angle tracking and error result.



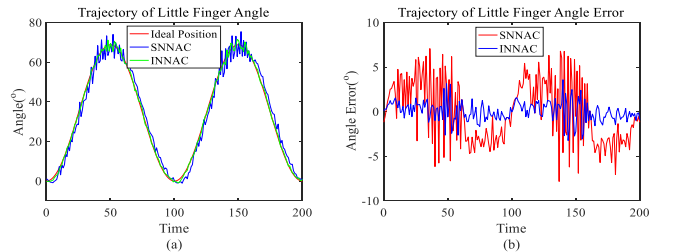Fig. 7. Ring finger angle tracking and error result.



Fig. 8. Little finger angle tracking and error result.

Table II shows the maximum angle error of the five fingers under the two control algorithms. It can be seen that the maximum angle error of INNAC is significantly reduced compared to SNNAC. The maximum angle error of the five fingers are respectively reduced by $4.659°$, $3.9418°$, $3.9844°$, $4.3958°$, $4.5173°$. The maximum angle error of the thumb is reduced by 59.6%, the index finger is reduced by 49.78%, the middle finger is reduced by 57.17%, the ring finger is reduced by 56.89%, and the little finger is reduced by 57.57%. Although the control effect of each finger is slightly different, but from the overall error trajectory of each finger, it can be seen that the error fluctuation of INNAC is smaller and the error range is closer to zero. Not only the control accuracy is improved, but the control jitter is smaller and the system is more stable.

TABLE II.　MAXIMUM FINGER ANGLE ERROR($°$)

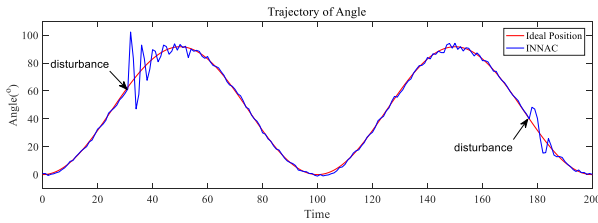|  | Thumb | Index Finger | Middle Finger | Ring Finger | Little Finger |
|---|---|---|---|---|---|
| SNNAC | 7.8169 | 7.9184 | 6.9690 | 7.7265 | 7.8462 |
| INNAC | 3.1579 | 3.9766 | 2.9846 | 3.3307 | 3.3289 |



Fig. 9.　Angle tracking results under external interference.

In the actual rehabilitation process, there may be various external disturbances. In order to verify that the designed scheme has strong stability and anti-interference ability. As shown in Fig. 9, with the middle finger as the experimental object, during the angle trajectory control process, external interference was artificially added during the bending and extension phases of the middle finger. It can be seen from the experimental results that at the moment of adding external interference, the control curve has a large oscillation, and then the oscillation gradually decreases until the normal trajectory tracking control is restored. And the smaller the external interference, the faster the recovery to normal speed. This experiment proves that the control method has good stability and anti-interference ability.

## V. CONCLUSION

In this paper, an INNAC method is proposed to control the bending angle of each finger of a hand rehabilitation robot driven by FPMs. In the actual experimental platform, the angle trajectory tracking control experiments were carried out for five fingers respectively, and the anti-interference experiment was verified. Experimental results show that this method has better control effect than SNNAC. INNAC has better angle control effect and stability, and the overall control performance is also improved. Under the external interference, this method can also quickly return to the normal tracking state, and has good stability and anti-interference ability.

In the future, we plan to introduce human-robot interaction and force feedback. On the basis of angle control, force sensors will be added to provide real-time feedback on finger joint angle and force signal, so as to complete some more complex and delicate rehabilitation training tasks.

REFERENCES

[1] H. Satoh, T. Kawabata, and Y. Sankai, "Bathing Care Assistance with Robot Suit HAL," IEEE International Conference on Robotics and Biomimetics, 2009, pp. 498-503.

[2] World Health Organization, " Global Health Estimates 2016: Deaths by Cause, Age, Sex, by Country and by Region, 2000-2016," https://www.who.int/news-room/fact-sheets/detail/the-top-10-causes-of-death, 2018.

[3] H. W. Li, T. Zhang and Y. J. Feng. Application of Exoskeleton-based Lower Limb Rehabilitation Robot in Stroke Rehabilitation[J]. Chinese Journal of Rehabilitation Theory and Practice, 2017, 23(7):788—791.

[4] J. H. Hsiao, J. Y. Chang. Soft medical robotics: clinical and biomedical applications,challenges, and future directions[J]. Advanced Robotics,2019,33(21):1099-1111.

[5] S. Guo, F. Zhao, W. Wei, and W. Zhang, "Soft actuator for hand rehabilitation," in international conference on mechatronics and automation, 2015, pp. 2197-2202.

[6] H. Al-Fahaam, S. Davis. Novel soft bending actuator-based power augmentation hand exoskeleton controlled by human intention[J]. Intelligent Service Robotics, 2018,11(3):247-268.

[7] B. Wang, A. McDaid, M. Biglari-Abhari, T. Giffney and K. Aw. A bimorph pneumatic bending actuator by control of fiber braiding angle[J]. Sensors & Actuators: A. Physical, 2017,257:173-184.

[8] B. Wang, A. McDaid, T. Giffney, M. Biglari-Abhari and K. Aw. Design, modelling and simulation of soft grippers using new bimorph pneumatic bending actuators[J]. Cogent Engineering, 2017,4(1).

[9] M. Farag, N. Z. Azlan and M. H. Alsibai. Slippage detection for grasping force control of robotic hand using force sensing resistors(Conference Paper)[J]. ACM International Conference Proceeding Series 2019 Part F148262 P98-102.

[10] C. Chen, J. Huang, D. Wu, and Z. Song, "T-S Fuzzy Logic Control with Genetic Algorithm Optimization for Pneumatic Muscle Actuator," in International Conference on Modelling, Identification and Control (ICMIC), 2018.

[11] G. Alici, T. Canty, R. Mutlu, W. P. Hu and V. Sencadas. Modeling and Experimental Evaluation of Bending Behavior of Soft Pneumatic Actuators Made of Discrete Actuation Chambers[J]. Soft Robot, 2018,5(1):24-35.

[12] A. Girin, F. Plestan, X. Brun and A. Glumineau. High-order sliding-mode controllers of an electropneumatic actuator: Application to an aeronautic benchmark[J].IEEE Transactions on Control Systems Technology, 2009, 17(3): 633-645.

[13] S. Boudoua, M. Hamerlain, and F. Hamerlain, "Intelligent Twisting Sliding Mode Controller using Neural Network for Pneumatic Artificial Muscles Robot Arm," in International Workshop on Recent Advances in Sliding Modes, 2015.

[14] N. Wang, D. Q. Wang. Adaptive manipulator control based on RBF network approximation[C]. Chinese Automation Congress. IEEE, 2017: 2625 - 2630.

[15] R. M. Robinson, C.S. Kothera, R.M. Sanner and N.M. Wereley. Nonlinear control of robotic manipulators driven by pneumatic artificial muscles[J]. IEEE/ASME Transactions on Mechatronics, 2016, 21(1): 55-68.

[16] L. Lee, I. Li. Design and implementation of a robust FNN-based adaptive sliding-mode controller for pneumatic actuator systems[J]. Journal of Mechanical Science and Technology, 2016,30(1):381-396.